POLITECNICO DI TORINO
Repository ISTITUZIONALE

Advanced models for static and dynamic analysis of wing and fuselage structures

Original
Advanced models for static and dynamic analysis of wing and fuselage structures / Filippi, M., Pagani, A., Carrera, E., Petrolo, M., Zappino, E.. - ELETTRONICO. - (2012). (8th Pegasus-AIAA Student Conference Poitiers, France 11-13 April, 2012).

Availability:
This version is available at: 11583/2507416 since:

Publisher:

Published
DOI:

Terms of use:

This article is made available under terms and conditions as specified in the corresponding bibliographic description in the repository

Publisher copyright

(Article begins on next page)

20 June 2026

Advanced Models for Static and Dynamic Analysis of Wing and Fuselage Structures

M. Filippi*, A. Pagani†,
E. Carrera‡, M. Petrolo§ and E. Zappino¶
Politecnico di Torino, Corso Duca degli Abruzzi 24, 10129 Torino, Italy.

Recently, an hierarchical formulation based on the Carrera Unified Formulation (CUF) was introduced by adopting polynomial expansions of the displacement field above the cross-section of the structure. The finite element method was exploited to develop numerical applications by employing the principle of virtual displacements. In the CUF framework the finite element matrices and vectors are expressed in terms of fundamental nuclei whose forms do not formally depend on the order and the class of the model. Two classes of 1D higher-order models have been developed according to the CUF. The Lagrange Expansion (LE) models were built by means of four- (L4) and nine-point (L9) Lagrange-type polynomials. The Taylor Expansion (TE) models exploit N-order Taylor-like polynomials. The classical 1D models are obtained as special cases of TE. This paper proposes advanced 1D theories for static and dynamic analysis of aeronautical structures. A number of typical stiffened-shell structures were analyzed. Classical 1D (Euler-Bernoulli and Timoshenko) and refined models were implemented by exploiting the 1D CUF. Finite element models made with a commercial software were used for comparison purposes. Results have highlighted the enhanced capabilities of the present formulation which is able to detect solid and shell-like accuracies with significantly lower computational costs.

Nomenclature

$\boldsymbol{C}$	Material stiffness matrix
$\boldsymbol{D}$	Linear differential operator matrix
$\mathbf{q}_{\tau i}$	Nodal displacement vector
$\mathbf{u}$	Displacement vector
$\mathbf{u}_\tau$	Generalized displacement vector
F_τ	Cross-section function
L_{ext}	External work
L_{ine}	Work of the inertial loadings
L_{int}	Internal work
N	Order of the expansion above the cross-section for the TE models
N_i	Shape function
T	Number of terms of the expansion
u_x, u_y, u_z	Displacement components in the x, y and z directions
x, y, z	Coordinates reference system
Symbols	
$\boldsymbol{\epsilon}$	Strain vector
$\boldsymbol{\sigma}$	Stress vector
δ	Virtual variation

*Ph.D. Student, Department of Mechanical and Aerospace Engineering, matteo.filippi@polito.it
†Ph.D. Student, Department of Mechanical and Aerospace Engineering, alfonso.pagani@polito.it
‡Professor, Department of Mechanical and Aerospace Engineering, erasmo.carrera@polito.it, AIAA Member
§Research Assistant, Department of Mechanical and Aerospace Engineering, marco.petrolo@polito.it
¶Ph.D. Student, Department of Mechanical and Aerospace Engineering, enrico.zappino@polito.it

I. Introduction

AIRCRAFT structures are essentially reinforced thin shells. The so-called *semimonocoque* constructions are composed by three main components: skins (or panels), longitudinal stiffening members and transversal members. Skins have the function of transmitting aerodynamic forces and of acting with the longitudinal members to resist the applied loads. Stringers resist bending and axial loads above the skin. Finally, ribs are used mainly to maintain the cross-sectional shape and to redistribute concentrated loads within the structure.

Wings and fuselages are subject to many different types of mechanical and aerodynamic loads throughout their operational life. These loads give rise to vibration in structures, leading to structural fatigue, flutter and noise transmission. Many different approaches were developed in the first half of the last century for the determination of stress/strain fields in the structural components of wings and fuselages. These approaches are discussed in major works.[1,2]

In the classical Finite Element Method (FEM) framework, reinforced-shell structures are generally described as complex systems in which one-dimensional (rod/beam) and two-dimensional (plate/shell) structural elements are appropriately assembled. A number of works have shown the necessity of a proper simulation of the "linkage" between stiffeners and panel.[3,4,5] On the other hand, the 3D finite element models are usually implemented as soon as the wing's structural layouts are determined. Because of their complexity, solid models are commonly used only within optimization processes. In fact, despite the availability of ever cheaper computer power, these FEM models present large computational costs.

The present paper proposes a new approach in the analysis of complex aircraft structures. Higher order one-dimensional models, based on the Carrera Unified Formulation (CUF), are used. Different techniques can be employed to construct higher-order models to overcome the limitations of the classical beam theories by Euler-Bernoulli (EBBT) and Timoshenko (TBT). The first attempts dealt with the introduction of shear correction factors, such as in Ref. 6; works by Dinis, Camotim and Silvestre[7] and Silvestre[8] dealt with the buckling analysis of thin walled open/closed cross-section beams by means of the Generalized Beam Theory (GBT); Gruttmann, Sauer and Wagner[9] focused on composite beams; asymptotic methods exploit an asymptotic expansion of a characteristic parameter to build refined theories, such as in Ref. 10, where the VABS method was used; theories including shear deformation effects were presented by Song and Waas.[11]

Recently, CUF 1D models have been developed[12,13] and are based on a hierarchical formulation which considers the order of the theory as an input of the analysis. Two classes of CUF 1D models have been proposed: the Taylor-expansion class, hereafter referred to as TE, and the Lagrange-expansion class, hereafter referred to as LE. The TE class is based on N-order Taylor-like polynomial expansions, $x^i\, z^j$, of the displacement field above the cross-section of the structure (i and j are positive integers). The order N of the expansion is arbitrary and is set as an input of the analysis. Static[14,15] and free-vibration analyses[16,17] have shown the strength of CUF 1D models in dealing with arbitrary geometries, thin-walled structures and local effects. Moreover, asymptotic-like analyses leading to reduced refined models were carried out in Ref. 18. The Euler-Bernoulli (EBBT) and Timoshenko (TBT) classical beam theories can be derived from the linear ($N = 1$) Taylor-type expansion. The LE class exploits Lagrange polynomials to build 1D refined models. Different types of cross-section polynomial sets can be adopted: nine-point elements, L9, four-point elements, L4, etc. LE models only have pure displacement variables. Static analyses on isotropic[13] and composite structures[19] have revealed the strength of LE models in dealing with open cross-sections, arbitrary boundary conditions and in obtaining Layer-Wise descriptions of the 1D model. The finite element formulation is adopted to deal with arbitrary geometries, boundary conditions and loadings.

A number of significant problems dealing with reinforced-shell structures have addressed in the following. The paper is organized as follows: a brief description of the CUF is given in Section II; numerical results are provided in Section III; main conclusions are then outlined in Section IV.

II. Refined 1D Models

A brief overview on the theoretical model is provided in this section. The adopted coordinate frame is presented in Fig. 1. The transposed displacement vector is defined as

$$\mathbf{u}(x,y,z;t) = \left\{ \begin{array}{ccc} u_x & u_y & u_z \end{array} \right\}^T \tag{1}$$

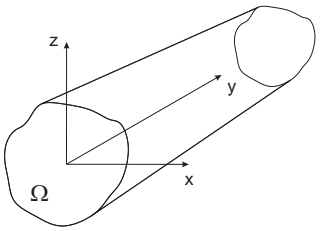

Figure 1. Coordinate frame of the beam model.

Stress, $\boldsymbol{\sigma}$, and strain, $\boldsymbol{\epsilon}$, components are

$$\boldsymbol{\sigma} = \left\{ \begin{array}{cccccc} \sigma_{xx} & \sigma_{yy} & \sigma_{zz} & \sigma_{xy} & \sigma_{xz} & \sigma_{yz} \end{array} \right\}^T, \quad \boldsymbol{\epsilon} = \left\{ \begin{array}{cccccc} \epsilon_{xx} & \epsilon_{yy} & \epsilon_{zz} & \epsilon_{xy} & \epsilon_{xz} & \epsilon_{yz} \end{array} \right\}^T \tag{2}$$

Linear strain-displacement relations were used,

$$\boldsymbol{\epsilon} = \boldsymbol{D}\mathbf{u} \tag{3}$$

where $\boldsymbol{D}$ is a linear differential operator whose explicit expression is not reported here for the sake of brevity, it can be found in Ref. 12.
Constitutive laws were exploited to obtain stress components,

$$\boldsymbol{\sigma} = \boldsymbol{C}\boldsymbol{\epsilon} \tag{4}$$

The components of $\boldsymbol{C}$ are the material coefficients. They can be found in Reddy.[20]

II.A. Unified Formulation

In the CUF framework, the displacement field is the expansion of generic functions, F_τ:

$$\mathbf{u} = F_\tau \mathbf{u}_\tau, \qquad \tau = 1, 2, ..., T \tag{5}$$

where F_τ vary above the cross-section. $\mathbf{u}_\tau$ is the generalized displacement vector and T stands for the number of terms of the expansion. According to Einstein notation, the repeated subscript, τ, indicates summation. The choice of F_τ determines which class of 1D CUF model to adopt.

The TE models are based on N-order Taylor-like polynomial expansions. For instance, the displacement component along the x-axis for the TE second-order ($N = 2$) refined 1D model is

$$u_x = u_{x_1} + x\ u_{x_2} + z\ u_{x_3} + x^2\ u_{x_4} + xz\ u_{x_5} + z^2\ u_{x_6} \tag{6}$$

On the other hand, LE models exploit Lagrange polynomials to refine 1D models. For example, the displacement component along x given by an L4 element is

$$u_x = F_1\ u_{x_1} + F_2\ u_{x_2} + F_3\ u_{x_3} + F_4\ u_{x_4} \tag{7}$$

Where $u_{x_1}, ..., u_{x_4}$ are the displacement variables of the problem and represent the translational displacement components along the x-axis of each of the four points of the L4 element.

Classical, refined and *component-wise* (CW) models can be implemented by means of CUF 1D. "Component-wise" means that each typical component of a reinforced-shell structure (i.e. stringers, sheet panels and ribs) can be modeled by means of a unique 1D formulation and, therefore, with no need for *ad hoc* formulations for each component. This methodology allows us to tune the model capabilities by 1. choosing which component requires a more detailed model; 2. setting the order of the structural model to be used. For more details about CW models see Ref. 21, 22.

II.B. Finite Element Formulation

The FE approach was adopted to discretize the structure along the y-axis. This process is conducted via a classical finite element technique, where the displacement vector is given by

$$\mathbf{u}(x, y, z; t) = F_\tau(x, z) N_i(y) \mathbf{q}_{\tau i}(t) \tag{8}$$

N_i stands for the shape functions and $\mathbf{q}_{\tau i}$ for the nodal displacement vector,

$$\mathbf{q}_{\tau i} = \left\{ \begin{array}{ccc} q_{u_{x_{\tau i}}} & q_{u_{y_{\tau i}}} & q_{u_{z_{\tau i}}} \end{array} \right\}^T \tag{9}$$

The explicit forms of the shape functions N_i, are not reported here, they can be found in the book by Bathe.[23]
The stiffness and mass matrices of the elements, and the external loadings that are coherent to the models were obtained via the Principle of Virtual Displacements:

$$\delta L_{int} = \delta L_{ext} - \delta L_{ine} \tag{10}$$

where L_{int} stands for the strain energy, L_{ext} is the work of the external loadings, and L_{ine} is the work of the inertial loadings. δ stands for the virtual variation. L_{int}, L_{ext}, and L_{ine} can be written as follows:

$$\delta L_{int} = \delta \mathbf{q}_{\tau i}^T \mathbf{K}^{ij\tau s} \mathbf{q}_{sj}, \qquad \delta L_{ext} = F_\tau N_i \mathbf{P} \delta \mathbf{q}_{\tau i}^T, \qquad \delta L_{ine} = \delta \mathbf{q}_{\tau i}^T \mathbf{M}^{ij\tau s} \ddot{\mathbf{q}}_{sj} \tag{11}$$

where $\mathbf{K}^{ij\tau s}$ and $\mathbf{M}^{ij\tau s}$ are the fundamental nuclei of the stiffness matrix and the mass matrix, respectively. $\mathbf{P}$ is a generic concentrated load. The nucleus components of $\mathbf{K}$ and $\mathbf{M}$ do not formally depend on the approximation order. This is the key point of the CUF which allows us, with only nine FORTRAN statements, to implement any-order beam theories. The derivation of the fundamental nuclei is not reported here for the sake of brevity, but it is in Carrera, Giunta and Petrolo,[12] together with a more detailed overview on the CUF.

III. Numerical Results

Static and free vibration analyses of typical aeronautical structures were performed and the results by 1D CUF models were compared to the results from MSC/NASTRAN© code. In the first part of this section the static analysis of a three-bay wing box is presented. The study carried out allows us to show the capability of the present refined 1D models of dealing with ribs and open sections. In the second part of this section the modal analysis of a fuselage structure is considered. Attention is focused on the capability of the present models of dealing with solid and shell-like FEM analyses with very low computational costs. Further results about wing and fuselage structures analyses can be found in Ref. 21, 22, 24.

III.A. Static Analysis of a Three-bay Wing Box

A static analysis of the wing structure presented in Fig. 2a was carried out. This structure consists of a three-bay box beam with a trapezoidal cross-section. The stringers were considered rectangular for convenience, however their shape does not affect the validity of the proposed analysis. Figure 2b shows the geometrical configurations of the multi-bay wing with no ribs and Fig. 2c shows the multi-bay beam with open mid-bay cross-section. These examples show the present advanced 1D models can accurately describe the effects due to ribs and open sections.

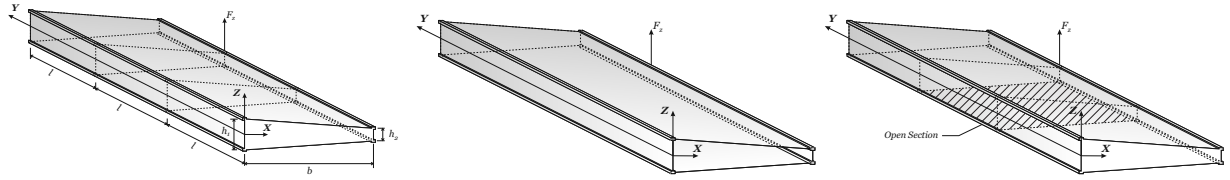

(a) Case 1: full model (b) Case 2: no ribs (c) Case 3: open mid-bay cross-section

Figure 2. The different structural configurations of the three-bay wing box.

Each bay had a length, l, equal to 0.5 $[m]$. The cross-section was a trapezium with height $b = 1$ $[m]$. The webs of the two spars were 1.6×10^{-3} $[m]$ thick, $h_1 = 0.16$ $[m]$ and $h_2 = 0.08$ $[m]$. The top and the bottom panels had a thickness of 0.8×10^{-3} $[m]$, as well as ribs. The area of the stringers was $A_s = 8 \times 10^{-4}$ $[m^2]$. The wing was made of an aluminium alloy 2024 with $G/E = 0.4$. The cross-section in $y = 0$ was clamped, whereas a point load, $F_z = 2 \times 10^4$ $[N]$, was applied at $[b, 2 \times l, h_2/2]$.

Table 1 shows vertical displacement values, u_z and the number of the degrees of freedom (DOFs) for each model. Results related to CUF models were validated by an MSC/NASTRAN© model built both with solid and shell FE elements (both stringers and ribs were discretized by means of solid elements, whereas shell elements were used for skins and webs). In Table 1, the increasing order Taylor-type models are considered in rows 4 to 7. N refers to the expansion order of the TE model. The LE model was implemented by discretizing the cross-section of each component as follows: stringers and panels/webs were composed by one L9 element each; the ribs were discretized with a combination of L4 and L9 elements.

Table 1. Displacement values, u_z, at loaded point and number of degrees of freedom for the three-bay wing box.

	Case 1, fig. 2a		Case 2, fig. 2b		Case 3, fig. 2c	
	$u_z \times 10^2$ [m]	DOFs	$u_z \times 10^2$ [m]	DOFs	$u_z \times 10^2$ [m]	DOFs
			MSC/NASTRAN©			
	1.412	100026	3.051	89400	1.963	89621
			Classical Beam Theories			
EBBT	0.464	495	0.464	495	0.464	495
TBT	0.477	495	0.477	495	0.477	495
			TE			
$N = 3$	0.793	1650	0.794	1650	0.873	1650
$N = 5$	1.108	3465	1.203	3465	1.500	3465
$N = 7$	1.251	5940	2.158	5940	1.745	5940
$N = 9$	1.325	9075	2.649	9075	1.836	9075
			LE			
	1.397	10750	2.981	10560	1.919	10446

Figures 3, 4, and 5 show the span-wise variation of axial and shear stress components for the three different structural configurations. A simplified analytical solution was considered for the full model (Fig. 2a) of the three-bay wing box for comparison purposes. This analytical solution can be found in Rivello.[2]

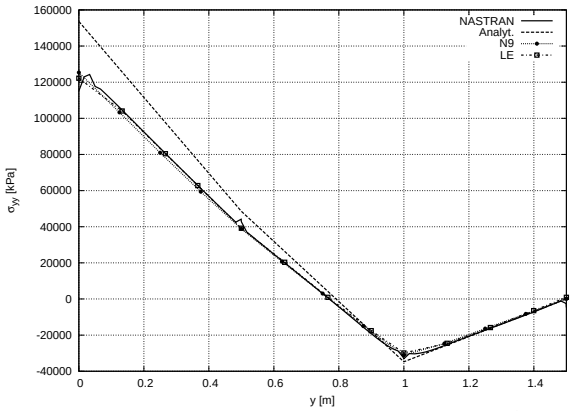

(a) Bottom right spar cap; σ_{yy} at $x = b$, $z = -\frac{h_2}{2}$

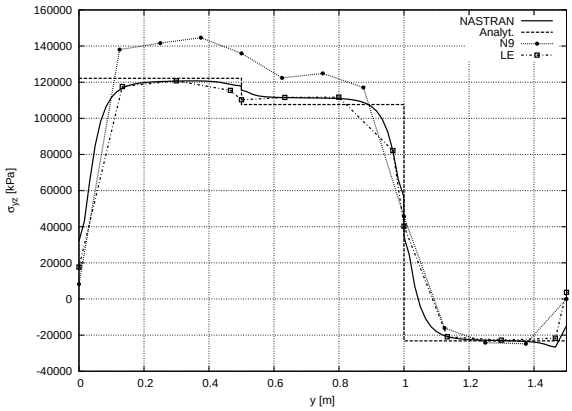

(b) Rear spar; σ_{yz} at $x = b$, $z = 0$

Figure 3. Stress components distribution along the wing span. Comparison of analytical, MSC/NASTRAN© and CUF models, case 1 (Fig. 2a).

Finally, Table 2 reports stress components values of both LE and MSC/NASTRAN© models. The following remarks can be made.

1. Refined beam theories, especially LE, allow us to obtain solid-like FEM accuracies.

2. The number of degrees of freedom of the present models is significantly reduced with respect to the MSC/NASTRAN© solid model (which is the most accurate and at the same time the most computational expensive).

3. Both the MSC/NASTRAN© and higher-order CUF models, unlike analytical theories based on idealized stiffened-shell structures and classical 1D models, allow us to highlight the effects due to ribs and open sections.

4. The Component-Wise capability of the present LE approach is clearly evident from the analysis conducted.

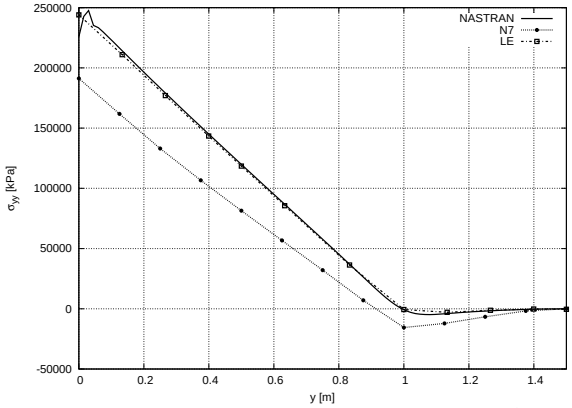

(a) Bottom right spar cap; σ_{yy} at $x = b$, $z = -\frac{h_2}{2}$

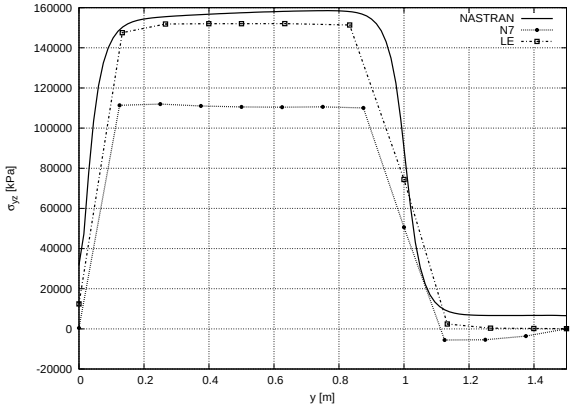

(b) Rear spar; σ_{yz} at $x = b$, $z = 0$

Figure 4. Stress components distribution along the wing span. Comparison of MSC/NASTRAN© and CUF models, case 2 (Fig. 2b).

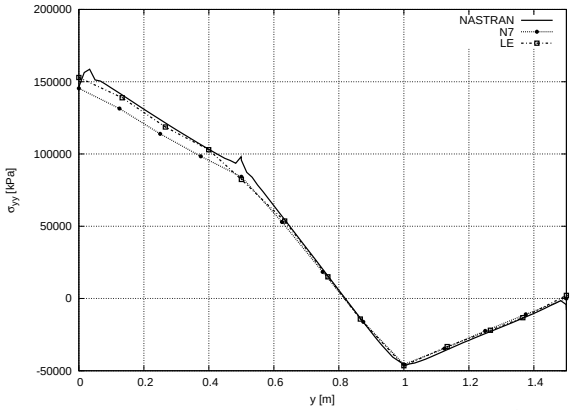

(a) Bottom right spar cap; σ_{yy} at $x = b$, $z = -\frac{h_2}{2}$

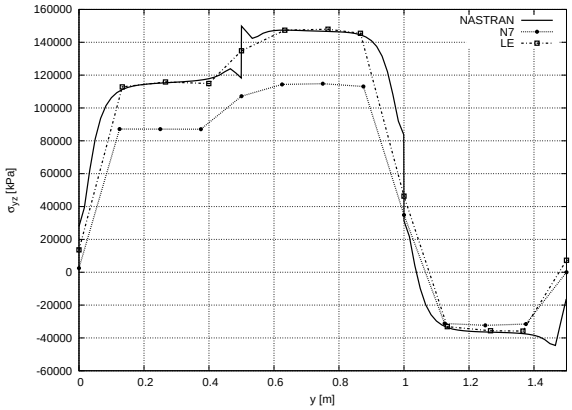

(b) Rear spar; σ_{yz} at $x = b$, $z = 0$

Figure 5. Stress components distribution along the wing span. Comparison of MSC/NASTRAN© and CUF models, case 3 (Fig. 2c).

Table 2. Stress components, σ_{yy} at $[b, \frac{l}{2}, -\frac{h_2}{2}]$ and σ_{yz} at $[b, \frac{l}{2}, 0]$, of the three-bay wing box.

	Case 1, fig. 2a		Case 2, fig. 2b		Case 3, fig. 2c	
Model	σ_{yy} [MPa]	σ_{yz} [MPa]	σ_{yy} [MPa]	σ_{yz} [MPa]	σ_{yy} [MPa]	σ_{yz} [Pa]
MSC/NASTRAN©	80.598	120.730	178.147	155.368	123.841	115.351
LE	80.404	120.603	177.018	151.876	118.684	115.810

III.B. Free Vibration Analysis of a Thin-walled Fuselage-like Cylinder

Modal analysis of a typical fuselage structure was carried out. The cross-section of the structure is shown in Fig. 6.

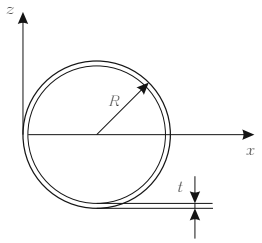

Figure 6. Thin-walled cylinder.

The longitudinal length, L, was equal to 15 $[m]$, and the radius, R, of the circular cross-section was 1 $[m]$. The thickness of the thin-walled cylinder was $t = 2 \times 10^{-3}$ $[m]$. The whole structure was made of isotropic aluminium alloy. The material data were: the Young modulus, E, was equal to 75 [GPa]; the Poisson ratio, ν, was 0.33; the density was $\rho = 2.7 \times 10^3$ $[Kg/m^3]$. Both of ends of the structure were clamped.

Table 3. Flexural and torsional frequencies of the skin. Comparison between different models.

	Frequencies $[Hz]$						
	$N = 1$	$N = 2$	$N = 3$	$N = 4$	$N = 5$	$N = 6$	MSC/NASTRAN©
$DOFs$	306	612	1020	1530	2142	2856	7800
F	50.656	51.458	46.590	46.531	46.510	46.499	46.951
	121.945	123.345	106.500	106.266	106.093	106.015	107.640
	209.589	211.282	177.589	176.826	176.696	176.675	179.360
T	105.874	105.874	105.874	105.874	105.873	105.873	108.590
	211.747	211.748	211.747	211.747	211.747	211.747	211.672
	317.621	317.621	317.621	317.621	*	*	317.102

* results not found in the first 60 frequencies.

Table 3 shows the frequencies of the first three flexural (F) and torsional (T) modes. Columns 2 to 7 report the results by the TE models. The CUF models were compared with an MSC/NASTRAN© model built with shell finite elements. It must be highlighted that when 1D CUF models are refined (by increasing the order of the expansion of the cross-section's displacement field, N) the frequencies converge to smaller values in agreement with the commercial code. Figure 7 shows the first three flexural modal shapes, whereas Fig. 8 the torsional modal shapes.

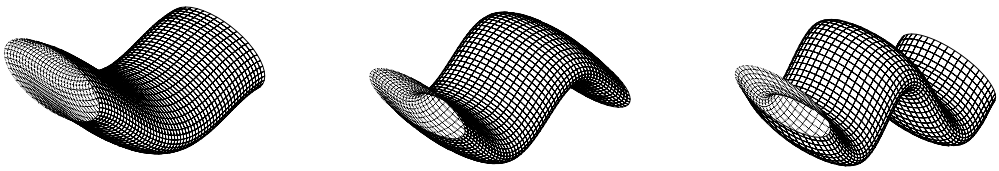

(a) $f = 46.590$ Hz (b) $f = 106.500$ Hz (c) $f = 177.589$ Hz

Figure 7. Flexural normal modes of the thin-walled cylinder. Cubic ($N = 3$) TE model.

Shell–like modes were detected using the TE higher-order models. These modes are modal shapes that involve wide cross-sectional deformations. The term "shell" is used to denote the fact that these type of modal shapes are usually detectable using plate/shell finite elements. The frequencies of the *shell–like* modes are reported in Table 4. L and M stand for the number of waves that can be identified in the longitudinal direction and cross-sectional direction, respectively. A cubic ($N = 3$) TE model was enough to predict the first *shell–like* modal shape. When the order of the interpolating TE polynomials is increased, the theory

Table 4. *Shell–like* mode frequencies. Comparison between different models.

Frequencies $[Hz]$						
		$N=3$	$N=4$	$N=5$	$N=6$	MSC/NASTRAN©
$DOFs$		1020	1530	2142	2856	7800
$L=1$	$M=2$	44.435	17.578	17.510	17.495	17.579
	$M=3$	*	52.871	10.534	9.808	9.409
	$M=4$	*	*	58.999	12.820	8.961
	$M=5$	*	*	*	64.023	12.450
$L=2$	$M=2$	97.414	44.987	44.905	44.889	45.244
	$M=3$	*	107.783	23.318	22.692	23.248
	$M=4$	*	*	117.294	18.115	15.473
	$M=5$	*	*	*	124.369	14.973
$L=3$	$M=2$	161.967	81.700	81.496	81.429	82.293
	$M=3$	*	167.330	44.599	44.141	43.479
	$M=4$	*	*	177.995	29.730	27.082
	$M=5$	*	*	*	186.547	21.028
$L=4$	$M=2$	237.043	124.579	124.061	123.964	125.470
	$M=3$	*	232.448	55.574	49.808	68.681
	$M=4$	*	*	241.501	45.836	42.633
$L=5$	$M=2$	320.597	171.417	170.252	170.098	172.290
	$M=3$	*	303.373	90.234	89.992	97.712
	$M=4$	*	*	*	68.892	61.385
$L=6$	$M=2$	410.699	220.504	218.278	217.973	217.228
	$M=3$	*	379.851	120.979	120.205	127.582
	$M=4$	*	*	*	97.772	81.577
$L=7$	$M=2$	505.844	306.466	266.254	266.063	264.763
	$M=3$	*	461.402	153.430	151.297	160.632
	$M=4$	*	*	*	136.764	104.651

* results not found in the first 60 frequencies.

becomes able to identify a larger number of modal shapes, while agreement between the MSC/NASTRAN© model and the TE models is improved. Some *shell–like* modal shapes are reported in Fig. 9. In conclusion, the analysis of the results suggest the following statements.

1. A linear TE model ($N=1$) is enough to correctly predict the torsional frequencies.
2. TE models which are higher than second-order are required to correctly detect the flexural frequencies, in accordance with MSC/NASTRAN©.
3. A TE model of at least a cubic order ($N=3$) is necessary to detect the *shell–like* modes. TE models which are higher than fourth-order provide good accuracy, and have a far lower number of degrees of freedom with respect to the MSC/NASTRAN© model.
4. By increasing the number of the expansion terms, the TE models identify even more *shell–like* modes which present a larger M.

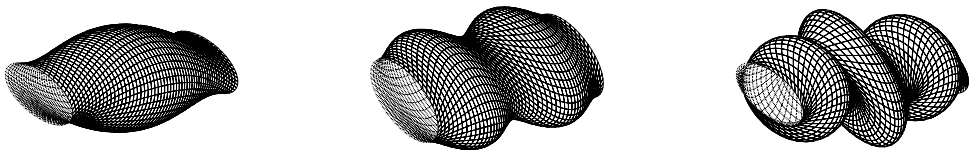

(a) $f = 46.590\ Hz$ (b) $f = 106.500\ Hz$ (c) $f = 177.589\ Hz$

Figure 8. Torsional normal modes of the thin-walled cylinder. Cubic TE model.

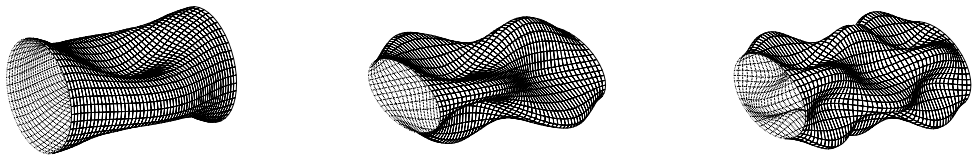

(a) $M = 2$, $L = 1$ (b) $M = 3$, $L = 2$ (c) $M = 4$, $L = 3$

Figure 9. $Shell - like$ **modal shapes corresponding to different values of** M **and** L**.**

IV. Conclusions

Two structural problems have been discussed in this paper, including multi-bay box wings and fuselage. Comparisons with solid and shell models from a commercial code were done. The results obtained suggest the following.

- The proposed refined 1D models offer a good level of accuracy in detecting the mechanical behavior of aircraft structures. In particular, torsional-bending couples, effects due to ribs and open sections, and shell-like modes are foreseen by increasing the order of the model.
- CUF 1D models allow us to deal with a large variety of complex wing structures, such as in Ref. 21,22, where the LE models are exploited with a CW approach.
- The present 1D formulation overcomes the need to combine different structural elements (beam, shell, etc.) to analyze thin-walled structures. In Ref. 24 CUF models were used for the analysis of complex fuselage configurations, including longitudinal and transversal stiffener members.
- The present formulation is extremely low in terms of computational costs compared to solid and plate/shell models. This aspect is of fundamental importance, since the design of an aircraft involves coupled problems (fluid-structure interaction) and it is often an iterative process.

Further work should be done on the structural analysis of a complete aircraft; the fuselage, the wing and the other lifting surfaces could be included in the same model by means of a unique 1D refined formulation.

References

[1]Bruhn, E. F., *Analysis and Design of Flight Vehicle Structures*, Tri-State Offset Company, 1973.

[2]Rivello, R. M., *Theory and analysis of flight structures*, McGraw-Hill, 1969.

[3]Vörös, G. M., "A special purpose element for shell-beam systems," *Computers and Structures*, Vol. 29, No. 2, 1988, pp. 301–308.

[4]M.S. Bouabdallah, J. B., "Formulation and evaluation of a finite element model for the linear analysis of stiffened composite cylindrical panels," *Finite Elements in Analysis and Design*, Vol. 21, 1996, pp. 669–682.

[5]Patel, S. N., Datta, P. K., and Seikh, A. H., "Buckling and dynamic instability analysis of stiffened shell panels," *Thin-Walled Structures*, Vol. 44, 2006, pp. 321–333.

[6]Jensen, J. J., "On the shear coefficients in Thimoshenko's beam theory," *Journal of Sound and Vibration*, Vol. 87, 1983, pp. 621–635.

[7]Dinis, P., Camotim, D., and Silvestre, N., "GBT formulation to analyse the buckling behaviour of thin-walled members with arbitrarily branched open cross-sections," *Thin-Walled Structures*, Vol. 44, 2006, pp. 20–38.

[8]Silvestre, N., "Generalised beam theory to analyse the buckling behaviour of circular cylindrical shells and tubes," *Thin-Walled Structures*, Vol. 45, 2007, pp. 185–198.

[9]Gruttmann, F., Sauer, R., and Wagner, W., "Shear stresses in prismatic beams with arbitrary cross-sections," *International Journal for Numerical Methods in Engineering*, Vol. 45, 1999, pp. 865–889.

[10]Cesnik, C. E. S., Sutyrin, V. G., and Hodges, D. H., "Refined theory of composite beams: the role of short-wavelength extrapolation," *International Journal of Solid Structures*, Vol. 33, No. 10, 1996, pp. 1387–1408.

[11]Song, S. J. and Waas, A. M., "Effects of shear deformation on buckling and free vibration of laminated composite beams," *Composite Structures*, Vol. 37, No. 1, 1997, pp. 33–43.

[12]Carrera, E., Giunta, G., and Petrolo, M., *Beam Structures: Classical and Advanced Theories*, John Wiley & Sons, 2011, DOI: 10.1002/9781119978565.

[13]Carrera, E. and Petrolo, M., "Refined Beam Elements with only Displacement Variables and Plate/Shell Capabilities," *Meccanica*, Vol. 47, No. 3, 2012, pp. 537–556, DOI: 10.1007/s11012-011-9466-5.

[14]Carrera, E., Giunta, G., Nali, P., and Petrolo, M., "Refined beam elements with arbitrary cross-section geometries," *Computers and Structures*, Vol. 88, No. 5–6, 2010, pp. 283–293, DOI: 10.1016/j.compstruc.2009.11.002.

[15]Carrera, E., Giunta, G., and Petrolo, M., *A Modern and Compact Way to Formulate Classical and Advanced Beam Theories*, chap. 4, Saxe-Coburg Publications, Stirlingshire, UK, 2010, pp. 75–112, DOI: 10.4203/csets.25.4.

[16]Carrera, E., Petrolo, M., and Nali, P., "Unified formulation applied to free vibrations finite element analysis of beams with arbitrary section," *Shock and Vibrations*, Vol. 18, No. 3, 2011, pp. 485–502, DOI: 10.3233/SAV-2010-0528.

[17]Carrera, E., Petrolo, M., and Varello, A., "Advanced Beam Formulations for Free Vibration Analysis of Conventional and Joined Wings," *Journal of Aerospace Engineering*, 2011, In Press, doi:10.1061/(ASCE)AS.1943-5525.0000130.

[18]Carrera, E. and Petrolo, M., "On the Effectiveness of Higher-Order Terms in Refined Beam Theories," *Journal of Applied Mechanics*, Vol. 78, No. 3, 2011, DOI: 10.1115/1.4002207.

[19]Carrera, E. and Petrolo, M., "Refined One-Dimensional Formulations for Laminated Structure Analysis," *AIAA Journal*, Vol. 50, No. 1, 2012, pp. 176–189, DOI: 10.2514/1.J051219.

[20]Reddy, J. N., *Mechanics of laminated composite plates and shells. Theory and Analysis*, CRC Press, 2nd ed., 2004.

[21]Carrera, E., Pagani, A., and Petrolo, M., "Classical, Refined and Component-wise Analysis of Reinforced-Shell Wing Structures," 2012, Submitted.

[22]Carrera, E., Pagani, A., and Petrolo, M., "Component-wise Method Applied to Vibration of Wing Structures," 2012, To be Submitted.

[23]Bathe, K. J., *Finite element procedure*, Prentice hall, 1996.

[24]Carrera, E., Filippi, M., and Zappino, E., "Free Vibration Analysis of Thin-Walled Structures with Longitudinal and Transversal Stiffeners," 2012, To be Submitted.